

# Experimental investigations of stimulated Brillouin scattering beam combination

David L. Carroll,\* Roosevelt Johnson, Shirley J. Pfeifer, and Richard H. Moyer

TRW, One Space Park 01/1210, Redondo Beach, California 90278

Received December 5, 1990; revised manuscript received July 23, 1992

We conducted an experimental investigation of beam combination of two beams by stimulated Brillouin scattering (SBS) to determine the conditions under which good phase locking, piston conjugation, and aberration correction could be achieved. Test parameters that were varied included bandwidth,  $f$ -number, near- and far-field separation between beams, power ratio between beams, beam aberrations, and polarization mismatch between the beams. The experiments were performed at 532 nm with  $n$ -hexane as the SBS medium. Piston-conjugation accuracy was measured by using fringe stability with conventional interferometry and by using extinction in a wave-front-reversing interferometer. The best piston conjugation was obtained when we maximized the overlap of the SBS interaction volumes of the two beams by minimizing the beam separation in the near and the far fields.

## 1. INTRODUCTION

Stimulated Brillouin scattering (SBS) not only produces a phase-conjugate beam that can be used to correct system aberrations<sup>1-3</sup> but also can be used to conjugate piston phase errors in multiple beams. In the SBS beam-combination geometry investigated in these experiments, two nearly parallel input beams are focused into a SBS cell. When the beams intersect in their SBS interaction regions near the focal plane, the acoustic Brillouin field that results is unique to the coherent superposition (including the relative phase) of the two optical beams; this uniqueness permits conjugation of not only the individual wavefronts but also the difference in the piston component of the two phases that would be caused by optical path mismatches. The diagnostics in our experiments measured the wave-front conjugation of each beam, the constancy of the piston phase difference between the two beams (denoted phase locking), and the elimination of the piston phase difference (denoted piston conjugation). Note that phase locking (obtained in some backseeded SBS geometries, for example) is a necessary but insufficient condition for piston conjugation.

Since the first verification of SBS beam combination by Basov *et al.*<sup>4</sup> there have been many experimental demonstrations and characterizations of the process. Vasil'ev *et al.*<sup>5</sup> showed that the maximum allowable angle between two beams coupled by SBS increases with pump power. Vasil'ev *et al.*<sup>5</sup> and Valley *et al.*<sup>6</sup> showed that the use of aberrators permits piston conjugation of misaligned beams by ensuring far-field overlap. Various investigators demonstrated the piston conjugation of multiple gain media: Rockwell and Giuliano<sup>7</sup> demonstrated piston conjugation with two Nd:YAG rod amplifiers, Gratsianov *et al.*<sup>8</sup> conjugated piston error in three Nd:glass slabs, and Leontev *et al.*<sup>9</sup> demonstrated piston conjugation of five Nd:glass rods and seven Nd:YAG amplifiers. Moyer *et al.*<sup>10</sup> quantified the requirements for far-field separation for effective piston conjugation as a function of focus-

ing  $f$ -number. Here we extend the SBS beam-combination database by reporting the results of tests intended to determine the conditions under which good piston conjugation and aberration correction could be achieved and to identify the underlying phenomena governing the process.

The SBS beam-combination experiments reported here address a number of effects, including the effects of laser bandwidth,  $f$ -number, near-field separation (NFS) and far-field separation (FFS) of beams, power ratio between the beams, beam aberrations, and (spatially uniform) polarization mismatch between the beams. In the case of narrow-band pump beams the location of highest SBS gain, called the SBS interaction region, is typically three times the Rayleigh range (established by the focusing  $f$ -number) of the beams.<sup>11</sup> A broadband laser reduces the SBS interaction region to an extent comparable with the laser coherence length; as a result, it is correspondingly more difficult to align the input beams to intersect in that region. The use of a broadband laser, therefore, would result in tighter alignment tolerances for the input beams, as is verified in the tests reported here. These tests also determined the effects of the geometry of beam overlap: Separating the beams in the near field reduces the volumetric overlap of the SBS interaction regions of the beams, and separating the beams in the far field moves the intersection point away from the focal plane to less intense regions of the beams. Tests with beams with highly unequal powers were performed; since the SBS interaction region is dependent on beam intensity, mismatched beams would show how changes in the position of the SBS interaction region affect requirements for intersecting the beams. The effects of beam aberrations were investigated to show the relaxation of beam alignment tolerances when the aberrated spot spread enhanced the overlap of the spots near the focal plane. Finally, the effects of the relative polarization state were assessed. Since orthogonally polarized beams do not interfere, and therefore could not set up a joint Brillouin acoustic field that is sensitive to the relative phase of the beams, it

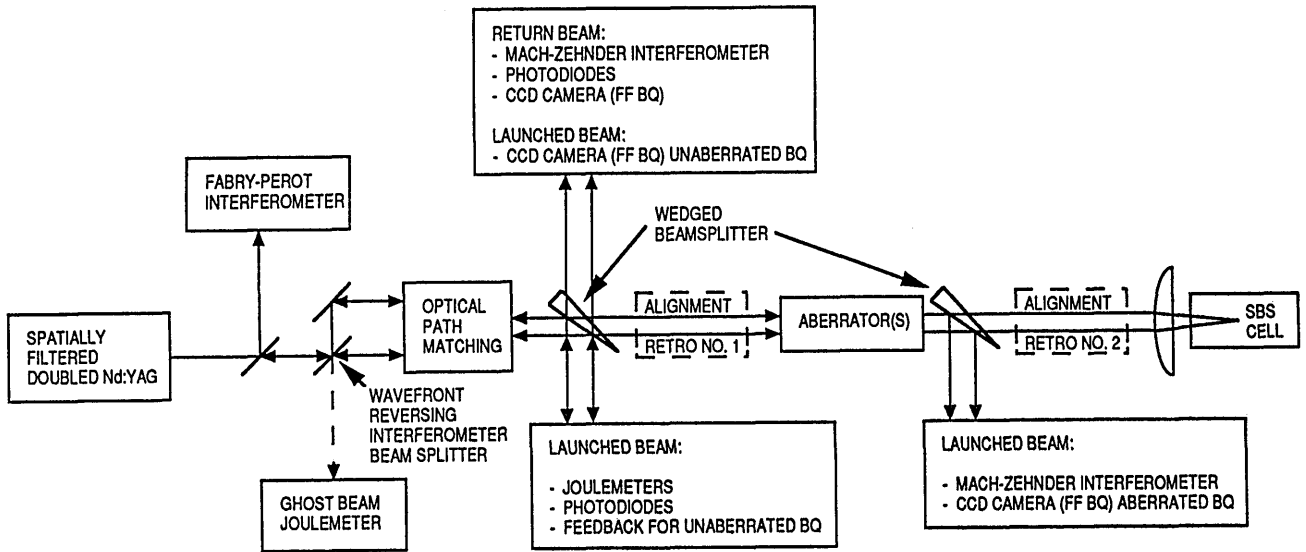


Fig. 1. Block diagram of the SBS beam-combination experiment. FF BQ, far-field beam quality.

would not be possible to conjugate piston errors between the beams. The tests reported here verify this effect and establish the tolerances for polarization matching.

These tests were performed with a frequency-doubled Nd:YAG laser focusing in *n*-hexane. The experiment diagnostics measured phase locking, piston error correction, and phase-conjugation fidelity for both single-shot tests and for the development of statistics for large numbers of shots. These diagnostics included a wave-front-reversing interferometer<sup>12</sup> that measured piston error correction and a Mach-Zehnder interferometer that measured both launched and return beams for phase-locking and phase-conjugation fidelity.

## 2. EXPERIMENTAL LAYOUT AND DIAGNOSTICS

A block diagram of the experiment is shown in Fig. 1. The output from the Moletron Nd:YAG laser, doubled to 532 nm, was spatially filtered and sent through near-field apertures to clip the resulting rings, yielding a laser pulse with a beam quality near unity (1.1 times the diffraction limit as measured in the far field by the CCD cameras, described below). The apertures were set at a diameter of 6.5 mm. A Glan-Taylor polarizer was used to polarize the beam linearly, and the rejected polarization was sent to a Fabry-Perot interferometer to measure the bandwidth of the launched beam. A beam splitter was used to split the beam into two for coupling in the SBS cell. The main beam splitter was a partial reflector, which was varied for different power ratios between the two beams. It also provided the basis for the wave-front-reversing interferometer described below. Optical path matching to within 1 mm was accomplished with a micrometer-adjusted translation stage.

Reflections from the first and the second wedged beam splitters were sent to launched- and return-beam diagnostics, which included joulemeters for measuring the energy of each launched beam, fast photodiodes for temporal profiles of both launched and return beams, Mach-Zehnder interferometers for near-field phase differences between beams in both pairs of launched and return beams (see

Fig. 2) and CCD cameras, which were used to measure the far-field beam quality of the unaberrated and the aberrated launched beams as well as the far-field beam quality of the phase-conjugate SBS return beams (Fig. 1). Beam quality was quantitatively measured by comparing the normalized far-field intensity distribution measured by the CCD cameras with the theoretical Airy intensity distribution. The aberrator plane was relay imaged through both of the Mach-Zehnder interferometers. Alignment checks were made with two flat reflectors on

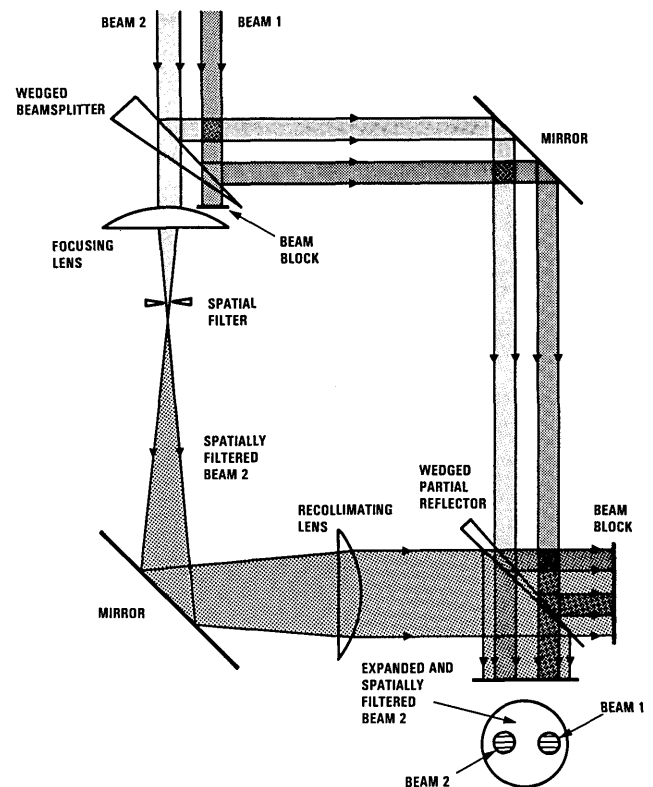


Fig. 2. Schematic of the Mach-Zehnder interferometers. Beams 1 and 2 interfere with a spatially filtered beam 2. Piston conjugation was monitored through fringe stability in beam 1.

kinematic bases (labeled RETRO NO. 1 and RETRO NO. 2 Fig. 1). The return-beam energy was computed based on the measured launched-beam energies and the average SBS reflectivity. The SBS cell used was 15 cm long (30 cm for the  $f/160$  tests) and filled with  $n$ -hexane. We isolated the laser oscillator from the SBS return by ensuring that the round trip was sufficiently long (200 ns) that the 15–20-ns laser pulse ended before the light could return to the laser.

When the SBS return beams recombine at the main wave-front-reversing interferometer beam splitter, the superposition of the two fields results in two beams emerging from the beam splitter: a beam traveling back toward the source laser (Fig. 3) and another beam, here denoted the ghost beam, which is directly related to errors in piston and wave-front conjugation. If the fields of the two SBS return beams (including piston error) were perfectly conjugated, they would constructively interfere in the direction of the source laser and destructively interfere in the direction of the ghost beam. This can be proved analytically by keeping track of phases and phase shifts at the beam-splitter-air interfaces or intuitively by recognizing that the time-reversal property of phase conjugation prohibits the return of a signal when there was no input. Thus perfect wave-front and piston conjugation yields zero power in the ghost beam; measurement of the Stokes return power at this point is a sensitive diagnostic method for detecting errors in the conjugation process. This diagnostic method is also sensitive to other effects, such as power mismatch from differences in the SBS reflectivity of the beams, wave-front mismatch from differences in the conjugation process, phase errors caused by optical path differences in the presence of the SBS frequency shift,<sup>4</sup> beam depolarization, beam misalignment and loss of overlap caused by bench jitter, and stray light resulting from optics scatter. Great care in the quantification and control of these sources of error was required for determination of piston-conjugation error from the wave-front-reversing interferometer. The relation between ghost-beam energy and piston error is obtained as follows: Start by assuming two uncorrelated fields input to the ghost-beam joulemeter,  $A_1(x, y, t)\exp[i\phi_1(x, y, t)]$  and  $A_2(x, y, t)\exp[i\phi_2(x, y, t)]$ , and define the phase difference (whether wave-front nonuniformity or piston error)  $\sigma(x, y, t)$  between the beams by the relation

$$\phi_2(x, y, t) = \phi_1(x, y, t) + 2\pi\sigma(x, y, t) + \pi. \quad (1)$$

The total energy  $E_g$  measured at the ghost-beam aperture is

$$\begin{aligned} E_g &= \int_0^\tau dt \int_{-a/2}^{a/2} dy \int_{-a/2}^{a/2} dx I(x, y) \\ &= \int_0^\tau dt \int_{-a/2}^{a/2} dy \int_{-a/2}^{a/2} dx |A_1 \exp(i\phi_1) + A_2 \exp(i\phi_2)|^2 \\ &= \int_0^\tau dt \int_{-a/2}^{a/2} dy \int_{-a/2}^{a/2} dx \\ &\quad \times \{A_1^2 + A_2^2 - 2A_1A_2 \cos[2\pi\sigma(x, y, t)]\} \\ &= E_1 + E_2 - 2 \int_0^\tau dt \int_{-a/2}^{a/2} dy \int_{-a/2}^{a/2} dx \\ &\quad \times \{A_1(x, y, t)A_2(x, y, t)\cos[2\pi\sigma(x, y, t)]\}, \end{aligned} \quad (2)$$

where  $E_1$  and  $E_2$  are the energies of the SBS return beams at the ghost-beam joulemeter. To simplify Eq. (2), we first assume that the average phase difference  $\sigma$  is time independent. Second, since the temporal profiles of the return beams have the same shape, as indicated by oscilloscope traces, we assume that  $A_1$  and  $A_2$  have the same functional dependence on  $t$ . Third, good conjugation fidelity ( $< \lambda/20$ ) was observed experimentally for both SBS return beams, so we assume that the most significant phase difference between the two return beams is caused by piston error, which is independent of  $x$  and  $y$ . Thus  $\cos(2\pi\sigma)$  can be brought out of the integral in Eq. (2). Based on the experimental observation of good conjugation fidelity of the SBS return beams and good overlap of the two return beams at the ghost-beam joulemeter, we assume perfect matching of the intensity profiles at the ghost-beam aperture. Thus the integral  $\int(dx dy A_1 A_2)$  reduces to  $(E_1 E_2)^{1/2}$ , and Eq. (2) becomes

$$E_g \cong E_1 + E_2 - 2(E_1 E_2)^{1/2} \cos(2\pi\sigma). \quad (3)$$

Solving for the piston error,  $\sigma$ , gives

$$\sigma = \frac{1}{2\pi} \cos^{-1} \left[ \frac{E_1 + E_2 - E_g}{2(E_1 E_2)^{1/2}} \right]. \quad (4)$$

Equation (4) is the relation between ghost-beam energy and piston error.

The wave-front-reversing interferometer, while difficult to implement, was the chief diagnostic tool for phase locking and piston conjugation; the simplicity of data recording (a joulemeter) made the interferometer indispensable for statistical analysis of large numbers of SBS beam-combination events. However, because of the assumptions made in arriving at Eq. (4), it is clear that small sources of ghost-beam energy other than piston error (such as wave-front mismatches) would cause a misinterpretation of the data; i.e., a ghost-beam power that indicates an error of  $\lambda/20$  may in fact be due entirely to wave-front nonuniformity. For this reason, to interpret the output of the diagnostics properly, we generated an error budget of quantifiable sources of spurious ghost-beam energy, shown in Table 1.

Included in Table 1 are the following nonrandom sources of error. First, the conjugation fidelity of each beam was measured to have a rms wave-front error of  $\lambda/20$  (determined with the FRINGE program, briefly discussed in Ref. 13). Second, the uncertainty of path matching between the two beams was approximately 1 mm, which translates into an error of  $\lambda/43$  in the presence of the Brillouin frequency shift<sup>4</sup> in  $n$ -hexane at 532 nm. Third, there was a 3° polarization matching uncertainty between

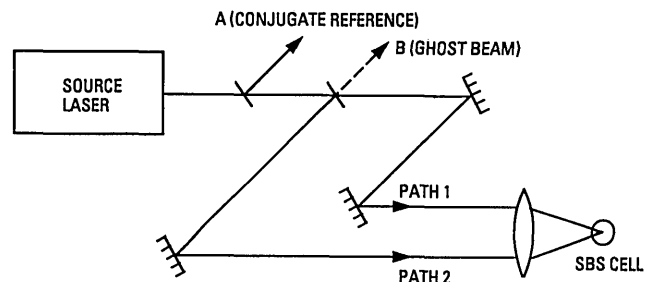


Fig. 3. Wave-front-reversing interferometer configuration.

**Table 1. Error Budget for the Ghost-Beam Diagnostics<sup>a</sup>**

Factors	Rms Error for Unaberrated Beams	Rms Error for Aberrated Beams
Ghost-beam offset factors		
Conjugation fidelity of beam 1	$\lambda/20$	$\lambda/10$
Conjugation fidelity of beam 2	$\lambda/20$	$\lambda/20$
Path mismatch (Brillouin frequency shift)	$\lambda/43$	$\lambda/43$
Depolarization	$\lambda/120$	$\lambda/120$
Scattered light	$\lambda/30$	$\lambda/30$
Ghost-beam results indicating at most $\lambda/30$ piston error	$\lambda/30$	$\lambda/30$
Total rms nonrandom offset error	$\lambda/11$	$\lambda/8$
Ghost-beam statistical scatter (broadening) factors		
Precision of three different joulemeters	$\pm\lambda/88$	$\pm\lambda/88$
Small fluctuations in SBS reflectivity relative to the average	$\pm\lambda/77$	$\pm\lambda/77$
Total rms statistical scatter	$\pm\lambda/58$	$\pm\lambda/58$
Total piston-conjugation error	$(\lambda/11 + \lambda/58) = \lambda/9$	$(\lambda/8 + \lambda/58) = \lambda/7$

<sup>a</sup>Including nonrandom offset and statistical scatter factors for unaberrated and aberrated experiments. The total piston-conjugation error is a convolution of these factors.

the beams at the ghost-beam joulemeter. If we assume two equal-energy beams that are out of phase by a half-wave at the ghost-beam joulemeter but have a linear polarization difference of  $3^\circ$ , the amount of energy in the perpendicular polarization state is approximately  $E \sin^2 \theta$ , where  $E$  is the energy of one of the beams and  $\theta$  is the polarization difference. When this amount of energy is used for the ghost-beam energy in Eq. (4) along with typical values for  $E_1$  and  $E_2$ , the resulting error is approximately  $\lambda/120$ . Fourth, scattered light (mostly backscatter from the SBS lens and the glass SBS cell that contains the *n*-hexane) was measured to contribute typically 0.018–0.024 mJ to the ghost-beam joulemeter reading. When this amount of energy is used for the ghost-beam energy in Eq. (4) along with typical values for  $E_1$  and  $E_2$ , the resulting effective error is approximately  $\lambda/30$ . Fifth, hereafter we define good piston conjugation to include shots that have at most  $\lambda/30$  piston error, so a  $\lambda/30$  piston error was included in Table 1. Since the measured quantity is the ghost-beam energy  $E_g$ , which is approximately proportional to the equivalent phase error squared (for phase errors less than  $\lambda/10$ ), the above equivalent phase shift errors were added as rms quantities, giving a total equivalent phase-shift error of  $\lambda/11$ . In addition, there were some random (statistical) sources of error as a result of the precision of the joulemeters and fluctuations in the SBS reflectivity. The joulemeters were accurate to  $\pm 5\%$  of their reading. The return-beam energy was computed based on the measured launched-beam energies and the average SBS reflectivity, which had measurement errors and variances, respectively, of approximately  $\pm 15\%$ . These variations were incorporated into Eq. (4) along with typical values for  $E_g$ ,  $E_1$ , and  $E_2$ ; the resulting rms sum of the individual contributions are given in Table 1. As shown in Table 1, the total piston conjugation error is  $\lambda/9$  ( $=\lambda/11 + \lambda/58$ ), indicating that any observed ghost-beam phase errors of  $\lambda/9$  or less are not likely to be the result of

a piston error of more than  $\lambda/30$ , whereas phase errors greater than  $\lambda/9$  are the result of poor piston conjugation. Good piston conjugation then refers to shots that have a ghost-beam phase error of at most  $\lambda/9$ .

To verify the consistency of the Mach-Zehnder and the wave-front-reversing interferometers in measurements of phase conjugation and piston conjugation, we made simultaneous measurements of the ghost-beam energy and of fringe movement and straightness of the return beams as measured by the Mach-Zehnder interferometer. Figure 4 shows that the two diagnostic methods agreed with each other to within the  $\pm\lambda/10$  data-reduction accuracy of Mach-Zehnder fringe movement.

## NARROW-BAND EXPERIMENTAL DATA

We conducted experiments on beam coupling with narrow-band input beams to determine the dependence of

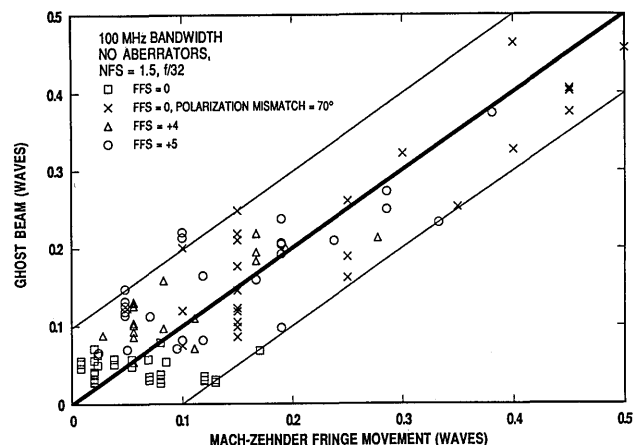


Fig. 4. Equivalent phase error of the wave-front-reversing interferometer ghost-beam energy compared with the Mach-Zehnder interferometer measurements.

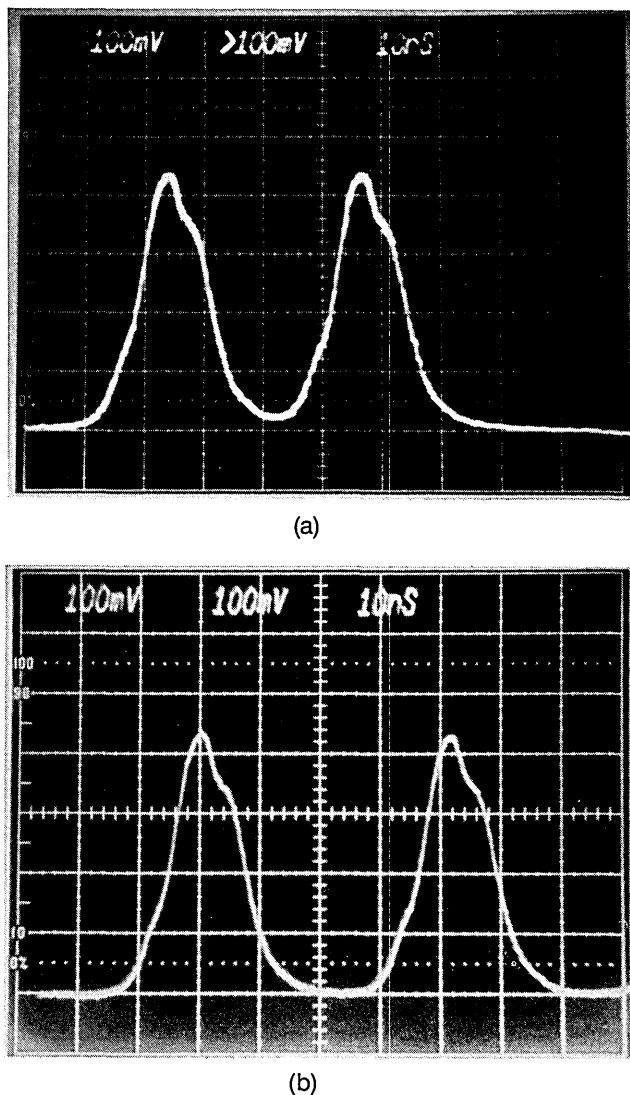


Fig. 5. (a) Launched and (b) SBS return profiles of both beams with the laser in 100-MHz operation.

phase locking on beam overlap (controlled by NFS and FFS) of unaberrated and aberrated launched beams, the energy ratio between beams,  $f$ -number, beam aberrations, and polarization mismatch. The narrow-band input beams were produced with the Nd:YAG laser operating on a single axial mode. Typical input and SBS return temporal profiles for both beams are shown in Fig. 5. The pulse duration FWHM was 15–20 ns. Fabry-Perot interferometer measurements showed the bandwidth to be  $100 \pm 10$  MHz. For  $f/32$  at 532 nm the SBS threshold for  $n$ -hexane with one beam was 0.15 mJ (10 kW) and with two beams maximally overlapped (FFS = 0, NFS = 1.5 beam diameters, center to center) was 0.12 mJ (8 kW) in each beam. Figure 6 shows SBS reflected power versus input power for both beams.

**A. Beam Coupling with No Aberrators**

The purpose of this experiment was to determine the ranges of NFS and FFS over which beam coupling can be achieved. Figure 7 shows the beam-coupling geometry with NFS in units of near-field beam diameter (6.5 mm) and FFS in units of the diffraction-limited spot diameter

(the diameter of the first zero of the Airy ring) at the focal plane. Both NFS and FFS are measured from the center of one beam to the center of the other. Negative FFS is defined to occur when the beams overlap upstream of focus and positive FFS to occur when the beams overlap downstream of focus. The fringe count in the Mach-Zehnder interferometer indicated the amount of tilt be

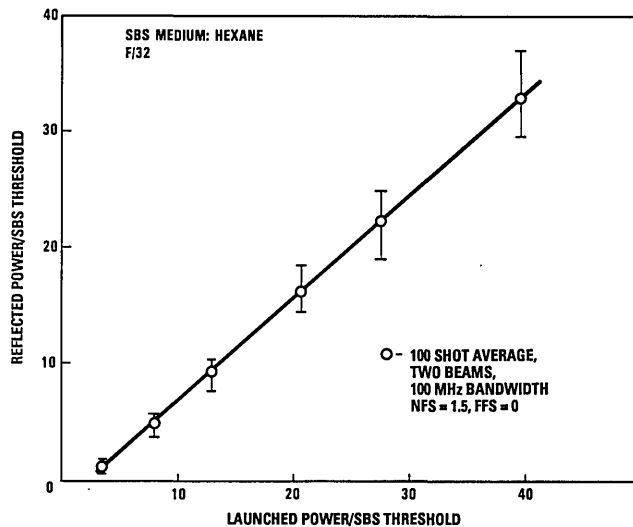


Fig. 6. SBS reflected power as a function of launched-beam power in 100-MHz operation.

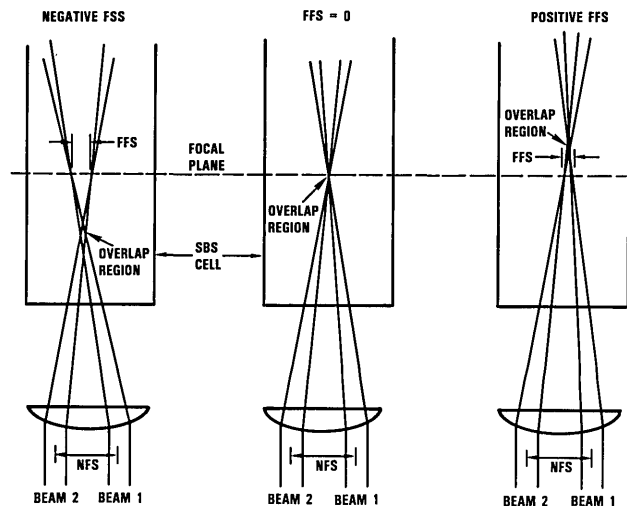


Fig. 7. Beam-coupling geometry.

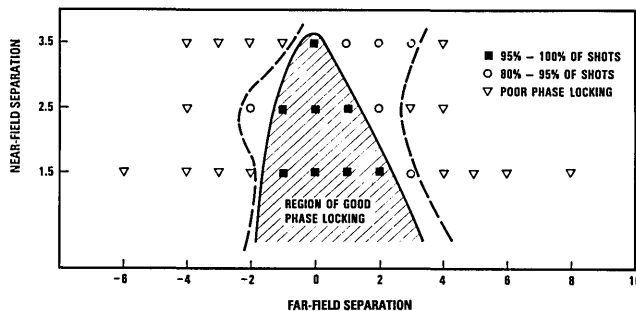


Fig. 8. Piston correction versus NFS (measured center to center in beam diameters) and FFS (measured in diffraction-limited spot diameters, i.e., Airy diameters) with unaberrated pump beams at 100 MHz.

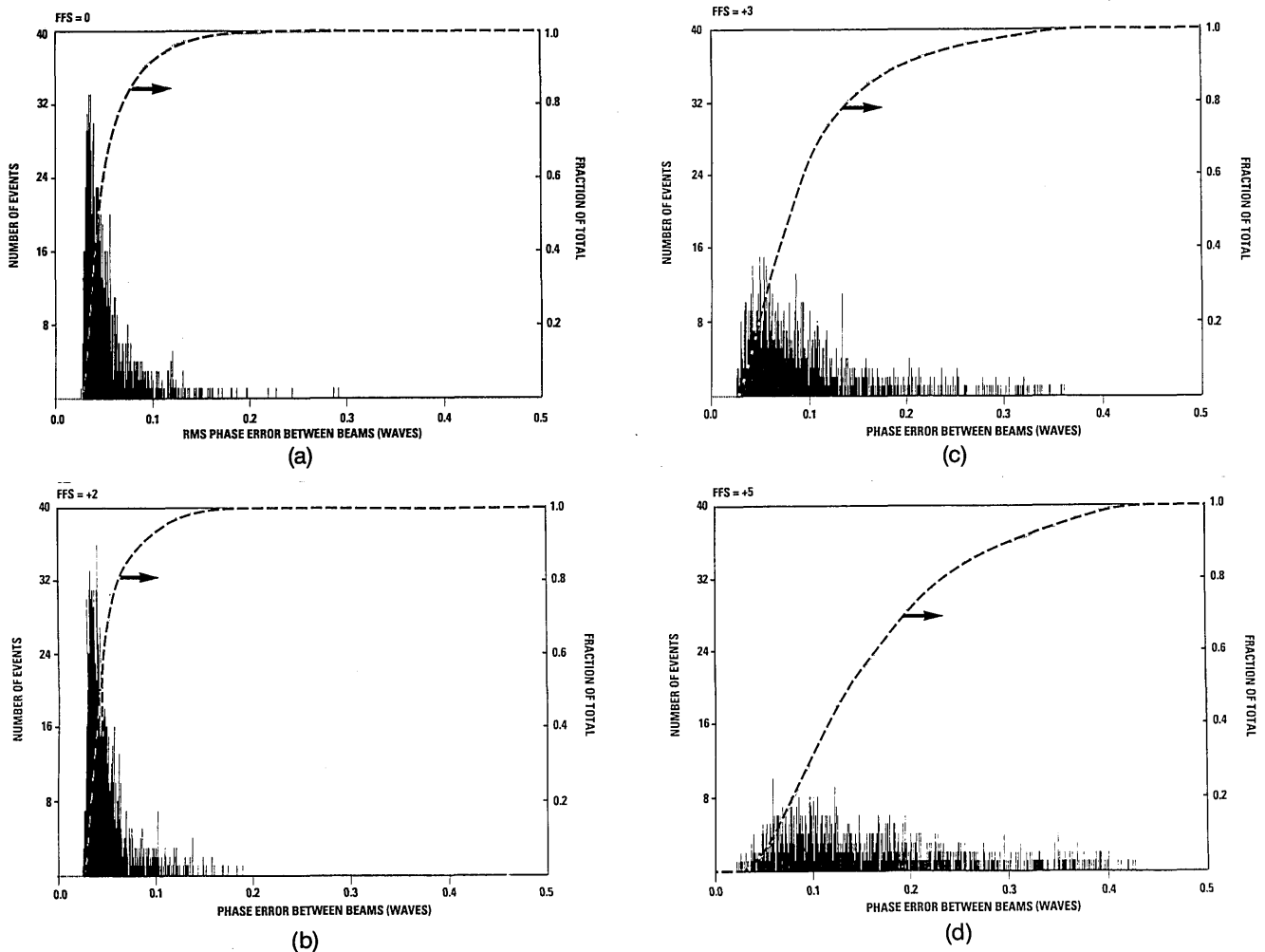


Fig. 9. Statistical data on piston correction for unaberrated pump beams at 100 MHz for far-field separations of 0, 2, 3, and 5 spot (Airy) diameters in (a), (b), (c), and (d), respectively. The dashed curves indicate the fractional number of pulses with less than the phase error indicated.

tween the beams; for every 2.44 fringes appearing in the interferometer, the focused spots in the SBS cell were separated by one diffraction-limited spot diameter.

Figure 8 shows a graph of beam coupling as a function of NFS versus FFS for the case of unaberrated beams. Beam coupling in Fig. 8 was determined from the ghost beam for a series of 25 consecutive shots (a few 100-shot samples were examined and gave the same results as 25-shot samples). The beam power was 11–17 times threshold. Good piston conjugation was achieved for NFS as large as 3.5. It was also observed that the most relaxed alignment tolerances were obtained at minimum NFS. For the case of unaberrated beams there was a slight tendency toward better coupling when the beams overlapped downstream of focus (for positive FFS); we have observed that this tendency was sensitive to aberrations in the beam. It should be noted that other reports of SBS beam combination (Lyubimov *et al.*,<sup>14</sup> Moyer *et al.*,<sup>10</sup> and Sternklar *et al.*<sup>15</sup>) indicate better performance with upstream overlap.

Statistics of ghost-beam energy measured with the wave-front-reversing interferometer were taken for 1000 consecutive laser pulses for 4 values of FFS at an NFS of 1.5. Raw data, as reduced by using Eq. (4), are illustrated

in Fig. 9; the histograms show a representative sample of the falloff in piston conjugation as the FFS was increased. Note that FFS's of 0 and +2 are similar in their distribution. Note also that, although FFS = +3 shows a broader distribution, approximately 85% of the shots are still coupled to within a  $\lambda/30$  piston error (e.g.,  $<\lambda/9$  overall, including ghost-beam errors; see Table 1). The fact that no shots in Fig. 9 show a piston conjugation of less than approximately  $\lambda/40$  is due to the always-present scattered light (Table 1). The fact that many of the shots for good coupling were observed to have an error of less than approximately  $\lambda/20$  rather than the given nonrandom offset of  $\lambda/11$  stated in Table 1 is probably the result of a combination of factors: First, the wave-front nonuniformities of  $\lambda/20$  for each beam may be working in a destructive way to minimize the ghost beam; second, the piston conjugation error may reduce the path mismatch error in the presence of the SBS frequency shift. Regardless of the cause of many shots' indicating phase errors of less than the nonrandom offset of  $\lambda/11$ , any observed ghost-beam phase errors of  $\lambda/9$  or less are not likely to be the result of a piston error of more than  $\lambda/30$ , whereas phase errors greater than  $\lambda/9$  are the result of poor piston conjugation.

Beam coupling as a function of vertical separation was

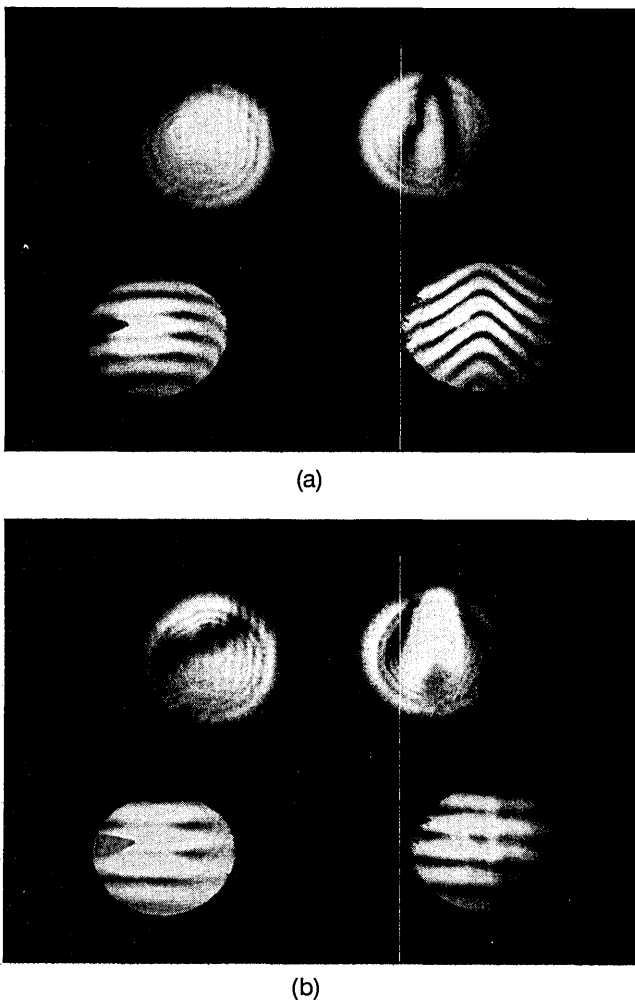


Fig. 10. (a) Launched and (b) SBS return near-field phase interferograms.

tested; locking was found to deteriorate rapidly when one of the beams was tilted out of plane instead of laterally. The reason for this loss of coupling is that the three-dimensional volumetric overlap between the beams is lost more rapidly when a beam is tilted out of plane than when the beam is merely translated along the other beam. Phase locking was lost when the vertical FFS was  $+0.5$ . However, two-dimensional arrays of beams may relax this pointing requirement. This sensitivity to out-of-plane misalignment was also observed by Sternklar *et al.*<sup>15</sup>

As can be seen from Figs. 8 and 9, the SBS beam combination process is statistically more effective when the beam overlap in the SBS interaction region is maximized. When two beams have no overlap in the SBS cell, the coupling between them should be completely random because the acoustic waves generated by each beam would not communicate.<sup>16-18</sup> Therefore it is reasonable to expect that there could be some randomness when the beams are weakly overlapped in the SBS interaction region. The randomness observed by Falk *et al.*<sup>19,20</sup> occurred at a NFS of 5, which produced a small volumetric overlap of the beams in the interaction region. Moyer *et al.*<sup>10</sup> reported piston conjugation within  $\lambda/15$  to  $\lambda/20$  wave accuracy 100% of the time for a small NFS of 1.1 (i.e., for strong overlap of the beams), which suggests that randomness in

the SBS beam combination is reduced as the beam overlap is increased. Figures 8 and 9 show that in the case of an intermediate NFS of 1.5–3.5 and a small value of FFS, 1–5% of the shots resulted in greater than  $\lambda/30$  piston conjugation error ( $>\lambda/9$  overall ghost-beam error). Possible causes of these shots with greater than  $\lambda/30$  piston error are jitter in the optical setup, reducing the overlap of the beams; breakdown in the SBS medium; or multimode laser pulses, which would degrade the SBS process (the latter two possibilities would account for only 1% of the bad shots at most, since the temporal profiles from shot to shot were carefully watched during the data-taking process).

### B. Beam Coupling with Applied Aberrations

The objective of this experiment was to determine the effect of pump-beam aberrations on the beam overlap requirements for piston conjugation. An additional objective was to detect the presence of cross talk, in which the aberrations of one pump beam, by means of the acoustic grating, may imprint onto an unaberrated pump beam in the coupling process. We performed these tests by placing a thin deformed microscope slide into beam 1 (as identified in Fig. 2) at the aberrator plane shown in Fig. 1. The aberrator plane was image relayed to the recording plane through both Mach-Zehnder interferometers. These tests were made with an  $f$ -number of 32, with each beam being 11–17 times threshold.

Figure 10 shows the launched and the return Mach-Zehnder interferograms of the aberrated beam 1 and the unaberrated beam 2. The corrected SBS return of the aberrated beam has a slightly reduced conjugation fidelity (approximately 0.10 rms waves) compared with that of the unaberrated return beam ( $<0.05$  rms waves). Figure 11 shows the far-field intensity distributions, recorded by the CCD camera, of the launched and SBS return beams. The far field of the aberrated launched beam displays two distinct peaks. It is believed that the weaker peak is not well reflected because it is only slightly above threshold, and thus the phase information representing the discontinuity is not fully reconstructed, as is seen in the return interferogram, Fig. 10(b). Data from the CCD camera showed that the far-field beam quality of the aberrated launched beam was 2.1 times the diffraction limit and that of the unaberrated launched beam was 1.1. The beam quality of the SBS-corrected return beam was 1.2, and that of the unaberrated return beam was 1.1. No evidence of transfer of the aberration from beam 2 to beam 1 was present.

Because of the degraded conjugation fidelity of the aberrated SBS return beam, the total nonrandom offset on the ghost beam was increased from  $\lambda/11$  to  $\lambda/8$ , which consequently increases the total piston conjugation error from  $\lambda/9$  to  $\lambda/7$  (Table 1). Hence, from our definition of good piston conjugation, ghost-beam results indicating at most  $\lambda/30$  piston error correspond to ghost-beam values of  $\lambda/7$  or less. Figure 12(a) shows piston conjugation with one aberrator as a function of NFS and FFS as indicated by the ghost-beam diagnostics. Figure 12(b) shows piston conjugation with one aberrator as a function of NFS and FFS as indicated by the fringe movement of the Mach-Zehnder diagnostics. Observe from Fig. 12 that the two diagnostic systems produce similar results but that the

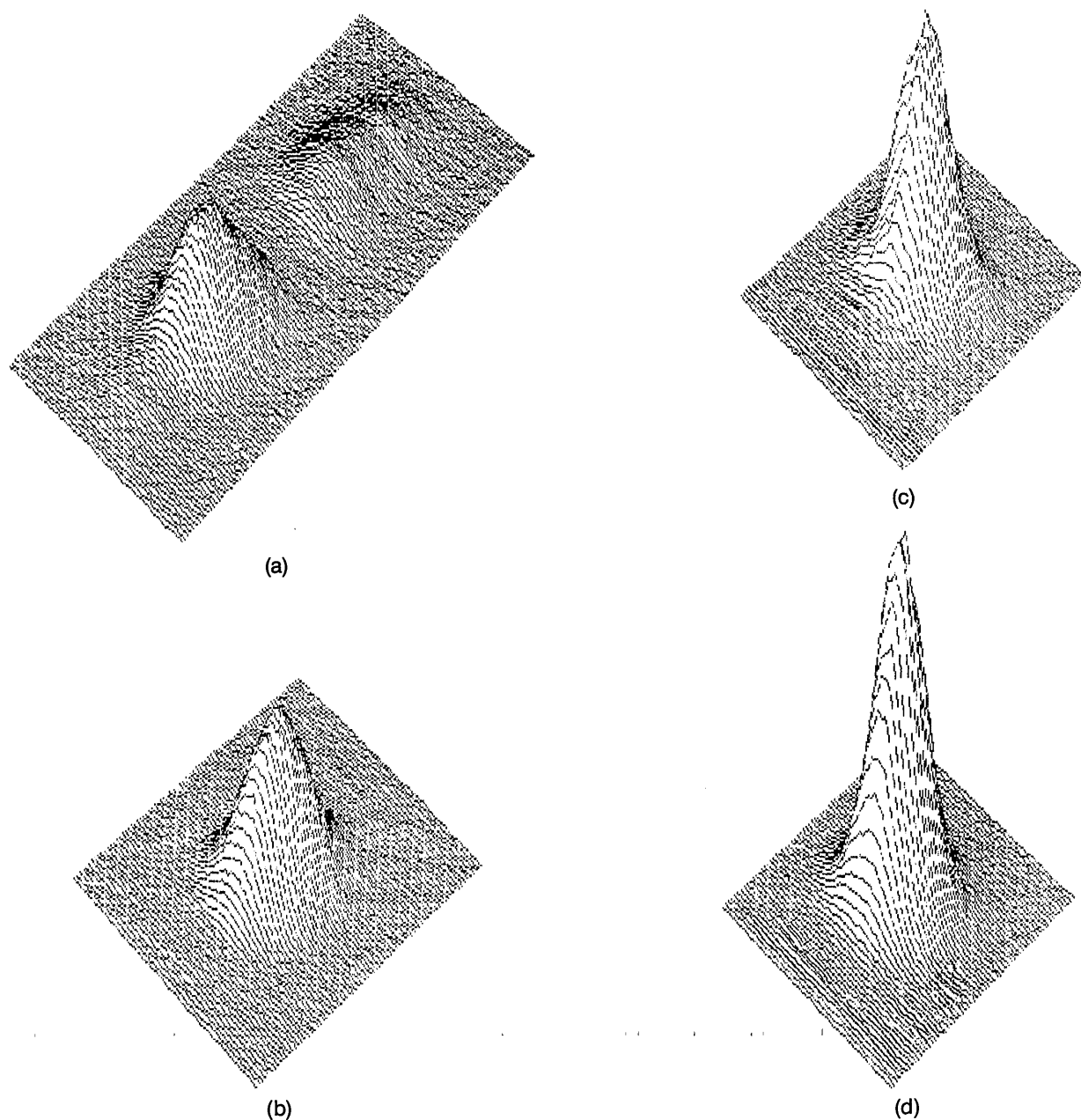


Fig. 11. Far-field intensity distributions from CCD camera beam-quality diagnostics. Shown are distributions for (a) the aberrated launched beam, (b) the unaberrated launched beam, and (c) and (d) the conjugated returns of beams 1 and 2, respectively.

wave-front-reversing interferometer is a more stringent test of piston conjugation, i.e., because of its less-precise method of data reduction, the Mach-Zehnder interferometer indicated a greater percentage of shots locked.

A significant result of this test is indicated by Fig. 12 as compared with the graphs of the unaberrated system (Fig. 8): aberrations increased the range of good beam coupling for both NFS and FFS, indicating that pointing tolerances are more relaxed for aberrated systems. For the smallest NFS the relaxation in the FFS tolerances should correspond to the increase in spot size caused by aberrations. Figure 12 shows a roughly twofold relaxation in the FFS tolerances, which is consistent with the approximate doubling of the far-field spot diameter shown in Fig. 11.

### C. Beam Coupling with Energy Balance Mismatch

The objective of this experiment was to determine the effect of unequal input beam powers on the ability of SBS to conjugate piston error. We varied the energy balance between the two beams entering the SBS cell by interchanging different partially reflective beam splitters for the wave-front-reversing interferometer (see Fig. 1); as a result, the sum of the two input beams' energies was a constant in these tests. These experiments were conducted with no aberrators, NFS = 1.5, and an  $f$ -number of 32. The results of these experiments, as determined from the ghost-beam diagnostics, are given in Fig. 13. It was found that good piston conjugation could be achieved for large energy mismatches. As can be seen, the piston-conjugation region was maintained down to energy ratios

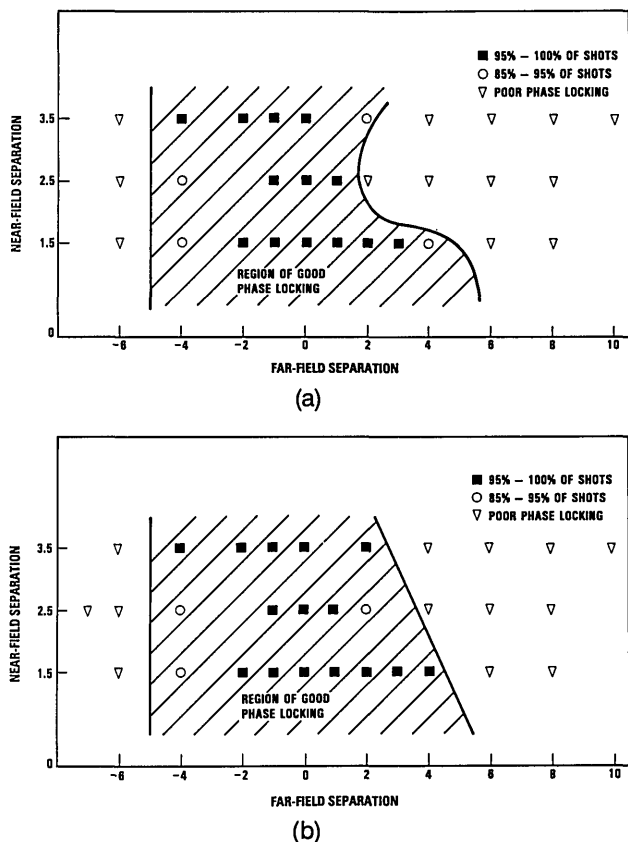


Fig. 12. Piston correction versus NFS and FFS with aberration in one pump beam (bandwidth, 100 MHz); results with (a) ghost beam and (b) Mach-Zehnder diagnostics.

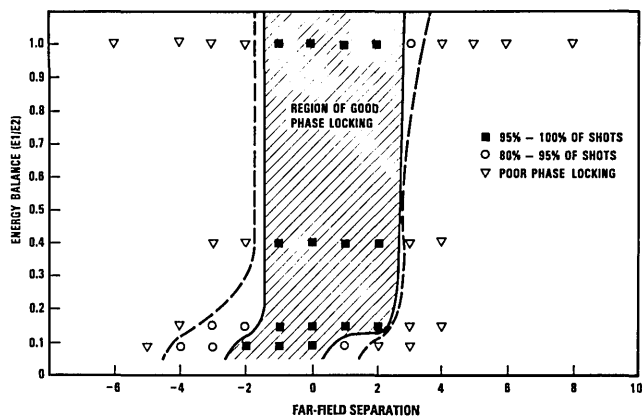


Fig. 13. Piston conjugation versus energy ratio between launched beams.

of 0.15. The shift in the coupling region at a power ratio of 0.1 is believed to be a consequence of the fact that the weak beam is only two times the SBS threshold. Thus the weak beam experiences much less pump depletion and would display low reflectivity in the absence of the other pump beam. Since the reflectivity of both beams is high, it may be inferred that the weaker beam is aided by the acoustic grating established by the strong beam. Since the strong beam is approximately 40 times threshold, it tends to conjugate in front of focus.<sup>14</sup> Thus the locking region moves upstream of focus for this condition.

### D. Beam Coupling with *f*-Number Variation

The objective of this experiment was to determine whether the *f*-number or the Rayleigh range plays a role in the SBS beam combination process. The *f*-numbers tested were *f*/32, *f*/80, and *f*/160, and we varied them by simply changing the lens that focused the two beams into the SBS cell. These tests were conducted with no aberrations and a NFS of 1.5, with each beam at 11–17 times threshold. The SBS threshold stayed approximately constant between *f*/32 and *f*/160, which is consistent with data taken by LeFebvre.<sup>21</sup> Figure 14 shows that good beam coupling was achieved between *f*/32 and *f*/160, as indicated by the ghost-beam diagnostic. A slight falloff in coupling range at *f*/160 was considered to be attributable to the 30-cm-cell length's limiting the crossing region of the two beams. In other words, because for every spot diameter separation in the far field the beams will overlap two Rayleigh ranges (one Rayleigh range was approximately 5 cm) away from focus, the beams will overlap outside the focally centered cell for |FFS| ≥ 2. The overall conclusion from these tests is that piston conjugation is nearly independent of *f*-number. Moyer *et al.*<sup>10</sup> obtained similar results for beam coupling as a function of *f*-number.

### E. Beam Coupling with Polarization Mismatch

The objective of this experiment was to evaluate the effect on beam coupling of mismatch between the spatially uniform polarization states of the two pump beams. It was demonstrated by Basov *et al.*<sup>22</sup> that conjugation fidelity is independent of polarization state, provided that the polarization is spatially uniform. We achieved a polarization mismatch at the SBS cell by placing a half-wave plate in beam 2 on its final path into the SBS cell. On reflection from the SBS medium the second pass through the half-wave plate resulted in the polarization's returning to the original state, regardless of the orientation of the half-wave plate. Thus the beams at the main beam splitter have the same polarization state and, in the presence of perfect conjugation, destructively interfere in the ghost-beam direction. Therefore any large ghost-beam readings indicate a piston error between the beams and not a polarization mismatch at the main wave-front-reversing interferometer beam splitter. The results from the ghost-beam diagnostics are given in Fig. 15, showing that good piston conjugation at the SBS cell was achieved for polarization mismatches of as much as 30° for greater than 90% of the shots and polarization mismatches of as

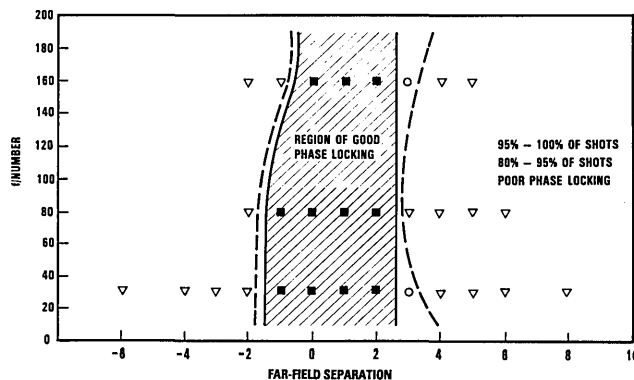


Fig. 14. Piston conjugation versus *f*-number at 100-MHz bandwidth.

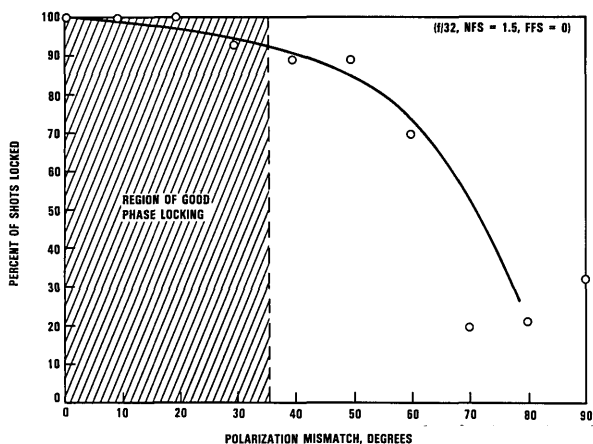


Fig. 15. Piston conjugation versus spatially uniform polarization mismatch.

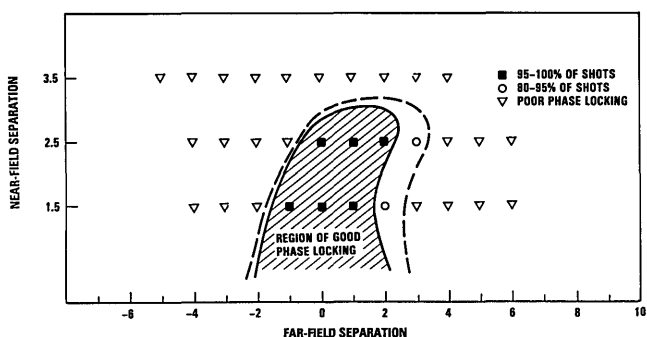


Fig. 16. Piston correction versus NFS and FFS with unaberrated pump beams at 15-GHz bandwidth.

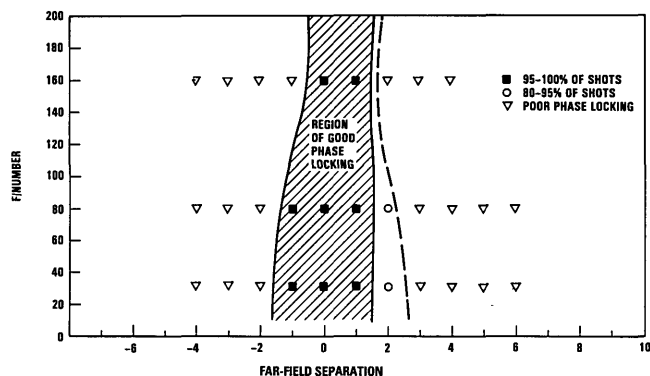


Fig. 17. Piston conjugation versus *f*-number at 15-GHz bandwidth.

much as 50° for greater than 80% of the shots. With polarization mismatches of less than 45°, the dominant projection of the polarization state of beam 2 is parallel to that of beam 1. It appears, then, that the correlation of the beams can be established. When the predominant polarization of beam 2 is orthogonal to that of beam 1, coupling is quickly lost because of the drop in the depth of interference that occurs between the two beams and a resultant decrease in the responsiveness of the acoustic field to the piston phase between the two beams. As can be seen, a substantial amount of polarization mismatch can be tolerated before piston conjugation between beams is degraded.

## BROADBAND EXPERIMENTAL RESULTS

Beam-combination data were collected by using a broadband (15-GHz) doubled Nd:YAG source. The broadband threshold was found to be approximately 15 kW, which is nearly twice the narrow-band threshold; this is consistent with data taken by LeFebvre.<sup>13</sup> Reflectivities of up to 62% were measured at pump powers of 38 times the broadband threshold. These reflectivities are somewhat lower than those measured in narrow-band operation.

### A. Beam Coupling

The experiment testing the dependence of beam coupling on FFS and NFS that was conducted at 100 MHz was repeated at 15 GHz. No applied aberrators were used, the *f*-number was 32, and each beam was 10–15 times the broadband threshold. Results for piston conjugation in the broadband regime, as determined by the ghost-beam diagnostics, are shown in Fig. 16. Comparison with Fig. 8 (narrow-band coupling without aberrations) shows that alignment tolerances are tighter for broadband than for narrow-band operation. Coupling was lost for NFS's greater than 2.5 beam diameters. The locking range in the far field is also seen to be somewhat reduced. This reduction is to be expected, since the shortened coherence length reduces the SBS interaction region; the range of angles over which one may aim the two beams while maintaining overlap within the interaction region is correspondingly limited.

### B. Beam Coupling with *f*-Number Variation

Experiments to determine the dependence of beam coupling on *f*-number were also repeated in broadband operation. These tests were performed with a NFS of 1.5, with each beam at 10–15 times the broadband threshold. The *f*-numbers tested were 32, 80, and 160, and the results, as determined by the ghost-beam diagnostics, are shown in Fig. 17. The trend is similar to that in narrow-band operation (Fig. 14). Piston conjugation was found to be nearly independent of *f*-number. Although the overall locking range is narrow at 15 GHz, it is preserved between *f*/32 and *f*/80. The 30-cm cell used for the *f*/160 tests may not have been long enough for FFS's greater than ±2. Thus better coupling at *f*/160 may be achievable with a longer SBS cell.

## CONCLUSIONS

SBS beam-combination experiments were conducted with a doubled Nd:YAG laser at 532 nm with band widths of 100 MHz and 15 GHz, pump powers to 40 times the SBS threshold, *f*-numbers from 32 to 160, varied polarization states, varied beam overlap in the SBS interaction region, with and without an aberrator, and varied energy ratios between beams. Good beam coupling was achieved for diffraction-limited pump beams with NFS's as large as 3.5 (at 100 MHz) and 2.5 (at 15 GHz) beam diameters and FFS's as large as 2 Airy diameters. The best piston conjugation was seen when the beam overlap in the SBS interaction region was maximized. The range of FFS over which piston conjugation occurred increased significantly in the presence of moderate aberrations in one of the pump beams. Good beam coupling was achieved for en-

ergy mismatches of as much as 10:1 when the weaker beam was at least twice the SBS threshold. Good beam coupling was achieved for a polarization mismatch between beams of up to 30°. FFS's out of the plane of crossing were limited to  $\pm 0.5$  Airy diameter for good piston conjugation.

## ACKNOWLEDGMENTS

We thank R. Aprahamian and M. Valley for several helpful discussions. We also thank J. Ho for his hard work in programming the computer software, which enabled us to utilize the CCD cameras fully as well as to take the statistics data.

\*Present address, Department of Aeronautical and Astronautical Engineering, University of Illinois, 104 South Mathews Street, Urbana, Illinois 61801.

## REFERENCES

1. D. M. Pepper, ed., special issue on nonlinear optical phase conjugation, *Opt. Eng.* **21**, 156–283 (1982).
2. R. A. Fisher, ed., *Optical Phase Conjugation* (Academic, New York, 1983).
3. B. Ya. Zel'dovich, N. F. Pilipetsky, and V. V. Shkunov, *Principles of Phase Conjugation* (Springer-Verlag, New York, 1985).
4. N. G. Basov, V. F. Efimkov, A. V. Kotov, A. B. Mironov, S. I. Mikhailov, and M. G. Smirnov, "Influence of certain radiation parameters on wavefront reversal of a pump wave in a Brillouin mirror," *Kvantovaya Elektron. (Moscow)* **6**, 765–771 (1979) [*Sov. J. Quantum Electron.* **9**, 455–458 (1979)].
5. A. F. Vasil'ev, A. A. Mak, V. M. Mit'kin, V. A. Serebryakov, and V. E. Yashin, "Correction of thermally induced optical aberrations and coherent phasing of beams during stimulated Brillouin scattering," *Zh. Tekh. Fiz.* **56**, 312–316 [*Sov. Phys. Tech. Phys.* **31**, 191–193 (1986)].
6. M. Valley, G. Lombardi, and R. Aprahamian, "Beam combination by stimulated Brillouin scattering," *J. Opt. Soc. Am. B* **3**, 1492–1497 (1986).
7. D. A. Rockwell and C. R. Giuliano, "Coherent coupling of laser gain media using phase conjugation," *Opt. Lett.* **11**, 147–149 (1986).
8. K. V. Gratsianov, A. F. Kornev, V. V. Lyubimov, A. A. Mak, V. G. Pankov, and A. I. Stepanov, "Investigation of an amplifier with a composite active element and a stimulated Brillouin scattering mirror," *Kvantovaya Elektron. (Moscow)* **13**, 2337–2339 (1986) [*Sov. J. Quantum Electron.* **16**, 1544–1546 (1986)].
9. V. M. Leontev, V. G. Novoselov, Yu. P. Rudnitskii, and L. V. Chernysheva, "Solid-state laser with a composite active element and diffraction-limit divergence," *Kvantovaya Elektron. (Moscow)* **14**, 364–368 (1987) [*Sov. J. Quantum Electron.* **17**, 220–223 (1987)].
10. R. H. Moyer, M. Valley, and M. Cimolino, "Beam combination through stimulated Brillouin scattering," *J. Opt. Soc. Am. B* **5**, 2473–2489 (1988).
11. J. Munch, R. F. Wuerker, and M. J. LeFebvre, "Interaction length for optical phase conjugation by stimulated Brillouin scattering: an experimental investigation," *Appl. Opt.* **28**, 3099–3105 (1989).
12. N. G. Basov, I. G. Zubarev, A. B. Mironov, S. I. Mikhailov, and A. Y. Okulov, "Laser interferometer with wavefront-reversing mirrors," *Zh. Eksp. Teor. Fiz.* **79**, 1678–1686 (1980) [*Sov. Phys. JETP* **52**, 847–851 (1980)].
13. M. LeFebvre, S. Pfeifer, and R. Johnson, "Dependence of stimulated-Brillouin-scattering phase-conjugation correction on the far-field intensity distribution of the pump light," *J. Opt. Soc. Am. B* **9**, 121–131 (1992).
14. V. V. Lyubimov, A. A. Mak, and V. E. Yashin, "Some problems in using wavefront reversal in laser systems," *Izv. Akad. Nauk SSSR Ser. Fiz.* **51**, 330–339 (1987) [*Bull. Acad. Sci. USSR Phys. Sci.* **51**, 330–339 (1987)].
15. S. Sternklar, D. Chomsky, S. Jackel, and A. Zigler, "Misalignment sensitivity of beam combining by stimulated Brillouin scattering," *Opt. Lett.* **15**, 469–470 (1990).
16. V. I. Bespalov, A. A. Betin, G. A. Pasmanik, and A. A. Shilov, "Observation of transient field oscillations in the radiation of stimulated Mandel'shtam-Brillouin scattering," *Pis'ma Zh. Eksp. Teor. Fiz.* **31**, 668–672 (1980) [*JETP Lett.* **31**, 630–638 (1980)].
17. M. V. Vasil'ev, A. L. Gyulameryan, A. V. Mamaev, V. V. Ragul'skii, P. M. Semenov, and V. G. Sidorovich, "Recording of phase fluctuations of stimulated scattered light," *Pis'ma Zh. Eksp. Teor. Fiz.* **31**, 673–677 (1980) [*JETP Lett.* **31**, 634–638 (1980)].
18. N. G. Basov, I. G. Zubarev, A. B. Mironov, S. I. Mikhailov, and A. Y. Okulov, "Phase fluctuations of the Stokes wave produced as a result of stimulated scattering of light," *Pis'ma Zh. Eksp. Teor. Fiz.* **31**, 685–689 (1980) [*JETP Lett.* **31**, 645–649 (1980)].
19. J. Falk, M. Kanefsky, and P. Suni, "Limits to the efficiency of beam combination by stimulated Brillouin scattering," *Opt. Lett.* **13**, 39–41 (1988).
20. J. Falk, Department of Electrical Engineering, University of Pittsburgh, Pittsburgh, Pennsylvania 15260 (personal communication, 1988).
21. M. LeFebvre, Thermo Electron Technology Corporation, San Diego, Calif. (personal communication, 1987).
22. N. G. Basov, V. F. Efimkov, I. G. Zubarev, A. V. Kotov, S. I. Mikhailov, and M. G. Smirnov, "Inversion of wavefront in SMBS of a depolarized pump," *Pis'ma Zh. Eksp. Teor. Fiz.* **28**, 215–219 (1978) [*JETP Lett.* **28**, 197–201 (1978)].